

# Dynamical Monte Carlo Study of Equilibrium Polymers (II): Effects of High Density and Ring Formation

A. Milchev<sup>1</sup>, J.P. Wittmer<sup>2\*</sup>, and D.P. Landau<sup>3</sup>

<sup>1</sup> *Institute for Physical Chemistry, Bulgarian Academy of Sciences,  
1113 Sofia, Bulgaria*

<sup>2</sup> *Département de Physique des Matériaux, Université Lyon I & CNRS,  
69622 Villeurbanne Cedex, France.*

<sup>3</sup> *Department of Physics and Astronomy, University of Georgia,  
Athens, Ga. 30602, U.S.A.*

## Abstract

An off-lattice Monte Carlo algorithm for solutions of equilibrium polymers (EP) is proposed. At low and moderate densities this is shown to reproduce faithfully the (static) properties found recently for flexible linear EP using a lattice model [1]. The molecular weight distribution (MWD) is well described in the dilute limit by a Schultz-Zimm distribution and becomes purely exponential in the semi-dilute limit.

Additionally, very concentrated molten systems are studied. The MWD remains a pure exponential in contrast to recent claims [2]. The mean chain mass is found to increase faster with density than in the semi-dilute regime due to additional entropic interactions generated by the dense packing of spheres.

We also consider systems in which the formation of rings is allowed so that both the linear chains and the rings compete for the monomers. In agreement with earlier predictions the MWD of the rings reveals a strong sin-

---

\*email:jwittmer@dpm.univ-lyon1.fr

gularity whereas the MWD of the coexisting linear chains remains essentially unaffected.

April 26, 2018

PACS numbers: 82.35.+t, 61.25H, 64.60C

## I. INTRODUCTION

The molecular mass distribution (MWD) of systems of linear unbranched “equilibrium polymers” (EP) is essentially exponential [1]. In EP systems polymerization takes place under condition of chemical equilibrium between polymer chains and their respective monomers. A classical example we will focus on is provided by systems of surfactants forming polydisperse solutions of long worm-like aggregates, called “giant micelles” (GM), which combine with each other, or break into smaller fractions [3].

Despite polydispersity, EP resemble in many aspects conventional quenched polymers where the polymerization reaction has been deliberately terminated. Recently, the basic scaling predictions for EP [3] based on classical polymer physics [4] have been tested by two of us (AM, JPW) [1] by means of a lattice Monte Carlo simulation based on the widely used Bond-Fluctuation Model (BFM) [5]. This demonstrated excellent agreement with theory over a very broad range of density and temperature variation. Specifically, it was shown that the MWD takes the form,

$$c(x)dx \propto \begin{cases} \exp(-x)dx & (N^* \gg \langle N \rangle, \phi^* \ll \phi) \\ x^{\gamma-1} \exp(-\gamma x)dx & (N^* \ll \langle N \rangle, \phi^* \gg \phi). \end{cases} \quad (1)$$

The scaling parameter  $x = N/\langle N \rangle$  is the ratio of the chain mass  $N$  and the mean mass  $\langle N \rangle$ ,  $N^*$  and  $\phi^*$  mark the mean mass and the density at the crossover from dilute to semi-dilute regimes at given scission energy  $E$ , and  $\gamma \approx 1.158$  is the susceptibility exponent of the  $n \rightarrow 0$  vector model in 3D [6]. The mean chain length  $\langle N \rangle$  was confirmed to vary with density  $\phi$  and the (dimensionless) scission energy  $E$  as

$$\langle N \rangle \approx N^* (\phi/\phi^*)^\alpha \propto \phi^\alpha \exp(\delta E) \quad (2)$$

with exponents  $\alpha_I = \delta_I = 1/(1+\gamma) \approx 0.46$  in the dilute and  $\alpha_{II} = (1+(\gamma-1)/(3\nu_I-1))/2 \approx 0.6$ ,  $\delta_{II} = 1/2$  in the semi-dilute regime. The exponent  $\nu_I \approx 0.588$  is the swollen chain (self-avoiding walk) exponent in 3D.

Recently, these results have been questioned in an interesting computational study where a reptation algorithm was used on a cubic lattice [2]. It was suggested that the MWD becomes singular  $c(N) \propto N^{-\tau}$  with  $\tau \approx 0.56$  at very high volume fractions of order unity. This finding, if corroborated, might be of some relevance in view of the alleged Levy-flight dynamic behavior in system of GM [7]. This claim prompted the present off-lattice Monte Carlo (OLMC) approach to be applied to the high density limit which was not accessible within our previous approach. We stress that effects only occurring at volume fractions of order one are unlikely to be relevant for real GM, but would be interesting on more general theoretical grounds in that the MWD in fact probes the free energy of the dense packing of beads.

As we are going to show, new physics (i.e. additional terms in the system free energy) intervenes indeed due to packing effects of the spherical beads. This increases effectively the growth exponent  $\alpha$  for  $\langle N \rangle$ , but does not effect the scaling form of the MWD. We do not observe any trace of singularity — in perfect agreement with the analytical predictions [3,8].

The investigation of the high density limit is only one motivation for the off-lattice algorithm proposed. In addition to this an effective OLMC for EP algorithm is highly warranted to overcome the usual shortcomings of lattice models and to serve in examining the role of polymers semi-flexibility. It is also a better tool in dynamic studies of a broader class of soft condensed matter systems where bifunctionality of the chemical bonds might be extended to polyfunctional bonds, as this is the case in gels and membranes. Note that the OLMC was already applied successfully to rheological properties of EP reported in [9] and to systems of EP brushes [10].

The scope of this paper is three-fold: we want to present the OLMC scheme and to test it by comparing the new results with previous findings (in the dilute and semi-dilute regime) obtained by means of our lattice Monte Carlo approach described in [1]. Secondly, we wish to address the physics in the melt density regime. In addition, the OLMC algorithm is tested in systems in which the formation of closed loops is allowed. We demonstrate for the first time in a computer experiment that there is a singularity of the ring MWD  $c_0(N) \propto N^{-\tau}$  where  $\tau = 5/2$  in 3D [11,12].

This paper is organized as follows. After presenting the algorithm in Sec.II we focus in Sec.III on the different density and chain length regimes reflected, e.g., by the distribution of the radius of gyration  $\langle R_g^2(N) \rangle$  versus mass  $N$  and other conformational properties. We discuss subsequently the MWD in Sec.IV. There we compare our OLMC results for mixed systems (in which rings are also present) with data obtained with the BFM and with a Grand Canonical lattice algorithm based on the mapping of the EP problem on a Potts model. The scaling of the mean chain mass is considered in Sec.V. The theoretical concepts (which have already been extensively considered elsewhere [3,8]) are briefly discussed *en passant*. We show that agreement of the OLMC with our previous work is excellent for small and moderate densities. For volume fractions larger 0.1 we evidence a third molten regime. In the final Section VI we summarize our findings.

## II. THE COMPUTATIONAL ALGORITHM

It is clear that in a system of EP where scission and recombination of bonds constantly take place the particular scheme of bookkeeping should be no trivial matter [13]. Since chains are only transient objects the data structure of the chains can only be based on the individual monomers, or, even better, on the saturated or unsaturated bonds [1]. This idea is depicted in Fig.1(a). Each bond is considered as a *pointer*, originating at a given monomer and pointing to the respective other bond with which the couple forms a nearest neighbor, or to *NIL* (nowhere), if the bond is free (unsaturated). Chains consists of symmetrically

connected lists of bonds:  $jbond = pointer(ibond) \leftrightarrow ibond = pointer(jbond)$ . Recombination of the two initially unsaturated bonds  $ibond = 2$  and  $jbond = 5$  connects the respective monomers  $imon = 2$  and  $jmon = 5$  in Fig.1(a). Note that only two pointers have to be changed and that the remaining chains behind both monomers are not involved. Breaking a saturated bond  $ibond$  requires resetting the pointers of the two connected bonds  $ibond$  and  $jbond = pointer(ibond)$  to *NIL*.

As mentioned in the Introduction this data structure has been incorporated [1] within the widely used BFM algorithm [5]. For the off-lattice version presented here we have now harnessed a very efficient bead-spring algorithm for polymer chains (for technical details see [14]) and cast it onto the data structure described above. This off-lattice Monte Carlo (OLMC) scheme is characterized by the bonded and the non-bonded interactions shown in Fig.1(b).

Each bond is described by a shifted FENE potential where a bond of length  $r$  has a maximum at  $r_{max} = 1$

$$U_{FENE}(r) = -K(r_{max} - r_0)^2 \ln \left[ 1 - \left( \frac{r - r_0}{r_{max} - r_0} \right)^2 \right] - E. \quad (3)$$

$E$  corresponds to a constant scission energy. Note that  $U_{FENE}(r = r_0) = -E$  and that  $U_{FENE}$  near its minimum at  $r_0$  is harmonic, with  $K$  being the spring constant, and the potential diverges logarithmically to infinity both when  $r \rightarrow r_{max}$  and  $r \rightarrow r_{min} = 2r_0 - r_{max}$ . Thus the FENE potential does not need to be truncated at  $r_{min}$  and  $r_{max}$  and discontinuities in the derivative of the potential are avoided. Following ref. [14] we choose the parameters  $r_{max} - r_0 = r_0 - r_{min} = 0.3$  and  $K/T = 40$ ,  $T$  being the absolute temperature. The units are such that the Boltzmann's constant  $k_B = 1$ .

The non-bonded interaction between effective monomers is described by a Morse-type potential,  $r$  being the distance between the beads

$$U_M(r) = \exp[-2a(r - r_{min})] - 2 \exp[-a(r - r_{min})] \quad (4)$$

with parameters  $a = 24$  and  $r_{min} = 0.8$ . The latter parameter sets roughly the sphere

diameter. The  $\Theta$ -temperature of the coil-globule transition for our model is  $\Theta \approx 0.62$  so that at  $T = 1$  we work under good solvent conditions [14].

The model can be simulated fairly efficiently with a dynamic MC algorithm, as described previously [14]. The trial update involves choosing a monomeric unit at random and attempting to displace it randomly by displacements  $\Delta x, \Delta y, \Delta z$  chosen uniformly from the interval  $-0.5 \leq \Delta x, \Delta y, \Delta z \leq 0.5$ . Moves are then accepted according to the Metropolis criterion and one Monte Carlo step (MCS) involves as many attempted moves as there are monomers in the system.

In equilibrium polymers the bonds between neighbors along the backbone of a chain are constantly subject to scission and recombination events. In the present model only bonds, stretched a distance  $r$  beyond some threshold value,  $r_b$ , are attempted to break so that eventually an energy  $U_{FENE}(r) > 0$  could be released if the bond breaks. Since each monomer may have at most two bonds in the same time, all particles with unsaturated bonds (two for single monomers and one for chain ends) may form new bonds, once they approach each other within the same interval of distances  $r_b \leq r \leq 1$  where scissions take place. (Note that recombination for  $r < r_b$  would violate detailed balance.)

We do not allow in the presented study for branching. However, more than two bonds per monomer are possible in principle and this feature may readily be included in the algorithmic framework. The generalization on netted structures like membranes or sponges is evident. (Note that this is less straightforward in the BFM scheme due to its lattice character which generates ergodicity problems.) Obviously, another big advantage of the off-lattice scheme compared to its lattice precursor is its applicability to rheological problems [10].

In most parts of this paper we focus on systems where no formation of ring polymers is allowed. This condition has to be observed whenever an act of polymerization takes place. Because there is no direct chain information in the data structure this has to be done by working up the list of pointers (which adds only four lines to the source code). In physical time units the simulation becomes *faster* for higher  $E$ : the number of recombinations per unit time goes like  $\exp(-E)$ , but the chain mass only grows as  $\exp(E/2)$ . Obviously, the

algorithm becomes even faster for the mixed systems discussed in Sec.IV B where the ring closure constraint has been dropped.

### III. CONFORMATIONAL PROPERTIES

The presented algorithm allows us to simulate a large number of particles at very modest expenses of operational memory. Most of the results in the present study involve 65536 particles for number densities between  $\phi = 0.125$  up to  $\phi = 1.5$ . Note that our highest densities correspond to very concentrated solutions. This can be better seen from the volume fractions which vary between  $v\phi \approx 0.03$  and  $0.33$ . The latter value has to be compared with the (only slightly larger) hard-sphere freezing volume fraction (“Alder transition”) of about one half [16] — it corresponds, in fact, to a relatively dense hard-sphere liquid. Note also that dense globules of maximal  $\phi \approx 2$  are formed by quenched monodisperse polymers in bad solvent [15].

The effective bead volume  $v \approx \pi l^3/6 \approx 0.22$  used above was estimated with the measured mean bond length  $l \approx 0.75$  from Tab.I. (Note that  $l$  is weakly decreasing with density [14] and that it is slightly smaller than the “bead diameter” given by the shifted Morse parameter  $r_{min}$ .) A similar, marginally larger volume of  $v \approx 0.25$  may be obtained from the virial expansion for quenched polymers [15].

The scission energy  $E$  was varied in a similar range as in [1] from  $E = 4$  up to  $E = 12$  to yield sufficiently strong chain mass variation. Note that the  $\langle N \rangle$  remains always two orders of magnitudes smaller than the total particle number within the box. Hence, from our previous study [1] one expects finite box-size effects to be small. This was indeed born out by finite-size test performed by varying the box sizes from  $16^3$  over  $32^3$  to  $64^3$ . Only the results from the largest boxes simulated for a configuration  $(E, \phi)$  are reported here.

Periodically the whole system is examined, the MWD  $c(N)$  (discussed in the subsequent section) and the distributions of the squared end-to-end distance  $\langle R_e^2(N) \rangle$  and gyration radius,  $\langle R_g^2(N) \rangle$  (averaged over all chains of a *particular* mass  $N$ ) are counted and stored.

(Periodic boundary conditions are implemented and interactions between monomers follow the minimum image convention. The computation of the conformational properties of the chains then imply a restoration of *absolute* monomer coordinates from the periodic ones for each repeating unit of the chain.) Moments obtained from these distributions are presented in Tab.I and Tab.II.

The different simulational regimes are most easily demonstrated by the conformational changes with density and chain mass. We demonstrate that the conformational properties for EP follow the same universal functions as conventional quenched polymers. In Fig.2  $\langle R_e^2(N) \rangle^{1/2}$  and  $\langle R_g^2(N) \rangle^{1/2}$  are plotted versus  $N$ . One configuration in the dilute regime and one in the concentrated limit (both at same  $E = 7$ ) have been presented. In the first case one clearly sees the swollen coil exponent. From the upper dashed line the persistence length of swollen EP is estimated as  $b = R_e/N^{0.588} \approx 0.92$ . In the latter case only chains smaller than the excluded volume blob of size  $\xi$  size are swollen. Larger chains ( $N \gg g$ ) show Gaussian behavior with  $R_e/\sqrt{6} \approx R_g \propto N^{1/2}$ . This slope was used to estimate the variation of the effective persistence length  $b = R_e/N^{0.5}$  with  $\phi$ . As can be seen from Tab.II  $b$  decreases with increasing density, hence with decreasing blob size  $\xi$  which we have estimated directly from the intercept of the two slopes at the radius of gyration. Note that  $\xi$  is relatively small for the densities computed.

The averages over all chains of the mean-square end-to-end distance  $R_e$  and the radius of gyration  $R_g$  are plotted versus  $\langle N \rangle$  in Fig.3. Swollen and Gaussian scaling behavior are again obtained for low and strong chain overlap respectively. Note that, e.g., the chains for  $\phi = 1$  are Gaussian for  $\langle N \rangle \geq 10$ . Thus the position of a particular configuration  $(E, \phi)$  with respect to the crossover from dilute to semi-dilute regime can be determined. This is consistent with the value  $\phi/\phi^*$  given in Table I where  $\phi^* = \langle N \rangle / (4\pi R_g^3/3)$  as usual.



## IV. MOLECULAR WEIGHT DISTRIBUTION

We focus first on systems without rings, as in the rest of the paper, and consider then the effects due to the ring closure constraint by allowing linear chains and rings to compete.

### A. Systems without rings

Fig. 4 displays a typical MWD  $c(N)$  obtained with the OLMC algorithm at high density ( $\phi = 1.5$ ). This is compared with BFM data. The  $c(N)$  is normalized such that  $\phi = \sum_N Nc(N)$ . Note that the free monomers are counted as chains of length  $N = 1$ . Both curves display to high accuracy nice exponentials. This is a generic result for strongly overlapping chains — even at extremely high volume fractions. Notably, at variance with a recent finding [2] no sign of singularity is observed.

In order to corroborate this result we try to scale the MWD obtained for different densities and scission energies. In Fig.5 we have plotted the (properly normalized) MWD versus the natural scaling variable  $x = N/\langle N \rangle$ . In the high density limit (main figure) data from two densities at various scission energies  $E$  (as indicated in the figure) collapses on a single ‘master distribution’  $c(x) = \exp(-x)$ . In the dilute limit, i.e. for the non-overlapping chains shown in the inset, we find again a data collapse, but with slightly different slope in linear-log coordinates. (Obviously, for large chain length the statistics deteriorates.)

How can these results be rationalized? Within a standard Flory-Huggins mean-field approach [3] one may write the total free energy density as

$$\Omega[c(N)] = \sum_{N=1}^{\infty} c(N) (\log(c(N)) + \mu N + f_{chain}(N, \phi, E)). \quad (5)$$

The first term on the right is the usual translational entropy. The second term entails a Lagrange multiplier which fixes the total monomer density  $\phi$ . The most crucial last term encodes the free energy of a reference chain of length  $N$  in the field created by the surrounding chains and free monomers.  $f_{chain}$  will in general depend on the chain length  $N$ , the density  $\phi$  and the bonded and non-bonded interaction parameters of the model studied [17]. We have

not computed here irrelevant additive terms (such as virial terms) which are not conjugated to  $c(N)$ . By functional derivation with respect to  $c(N)$  one readily obtains the equilibrium MWD:

$$c(N) = \exp(-E - f_{end}(N, \phi, E) - \mu N). \quad (6)$$

We have defined here  $f_{end} = f_{chain} - E - 1$  and absorbed all contributions to  $f_{end}$  linear in  $N$  within the Lagrange multiplier. Hence, within the mean-field approximation eq.(5) the MWD discussed above probes directly the free energy of an EP chain (besides the terms linear in  $N$  mentioned above which are fixed by the imposed density) which essentially “renormalizes” the scission energy  $E$ .

We infer from Fig.4 and Fig.5 that for our EP chains  $f_{end}$  is to very high accuracy mass independent. Two classical examples where this is indeed rigorously true are non-interacting rigid rods and Gaussian chains [3]. (There  $f_{end}$  is even independent of  $\phi$ .) If this is the case, the MWD becomes then a pure exponential

$$c(N)dN/\phi = c(x)dx = \exp(-x)dx \quad (7)$$

where the scaling variable is  $x = N/\langle N \rangle$ , i.e. the inverse Lagrange multiplier equals the mean-chain length,  $\langle N \rangle \mu = 1$ .

This is in agreement with our scaling in the high density limit which implies that  $f_{end}$  is within numerical accuracy independent of  $N$ . We have explicitly checked that here the MWD scales like  $c(N) \propto \exp(-E - f_{end}(\phi) - N/\langle N \rangle)$  where  $f_{end}$  only depends on  $\phi$ . The slightly different slope found in the dilute regime suggests, however, a weak mass effect. It is relatively simple to understand these results from the standard theory of polymers in good solvent solutions [1]. There the chemical potential of ends is given by  $f_{end} = (\gamma - 1)/\nu_I \log(\xi)$  where  $\xi$  is size of the ‘blob’, i.e. the excluded volume correlation length for chains of length  $N$  at density  $\phi$ .

In the semi-dilute limit we have  $\xi \propto g^{\nu_I} \propto \phi^{-\nu_I/(3\nu_I-1)}$  [4] ( $g$  denotes the number of monomers within a blob), hence

$$f_{end} = (\gamma - 1)/(3\nu_I - 1) \log(\phi/\phi_0) \quad (8)$$

is independent of mass and scission energy. The constant reference density  $\phi_0$  was introduced here for dimensional reasons. Obviously, eq.(8) can strictly hold only in the asymptotic limit of large blob sizes ( $\phi \rightarrow 0$ ). Additionally, one can not exclude weak chain-length dependence of  $f_{end}$  at  $N \approx 1$ , but this becomes irrelevant in the scaling limit of  $\langle N \rangle \gg 1$  [18].

In the opposite dilute limit the correlation length becomes density independent and is given by the size of the chain  $\xi = R \propto N^\nu$ . Hence,  $f_{end} = (\gamma - 1) \log(N)$  and the MWD becomes the Schultz-Zimm form given in the Introduction (eq.1). Note that the  $\gamma$ -exponent in 3D is only slightly larger than its mean field value  $\gamma = 1$ . Hence, the predicted power law depletion in the MWD for small  $N$  is very weak and requires a relatively large mean chain mass  $\langle N \rangle \gg 1$ . This is why within the range of the parameters accessible essentially only the slightly different exponential tail  $c(x) \propto \exp(-\gamma x)$  is visible.

Obviously, some of our simulations are in the intermediate regime ( $\phi \approx \phi^*$ ) between these limiting cases (depicted by the two slopes in Fig.5). In order to characterize all the MWD with one parameter we fitted the tail of  $\log(c(N))$  with  $-E - f_1 - \mu N$  where both  $\mu$  and  $f_1$  are fit parameters. In the dense limit naturally one finds  $\mu \langle N \rangle = \gamma_{eff} \approx 1$ . As soon as the overlap decreases  $\gamma_{eff} \rightarrow \gamma$ . Note that the  $f_1$ -variation with  $E$  for given  $\phi$  is weak and we have only tabulated the value for the highest  $E$ , i.e. for the most strongly overlapping chains. The values are given in Tab.II and are discussed in the subsequent Section V.

## B. Mixed systems with linear chains and rings

First we briefly assess the importance of the ring closure constraint. We allow the formation of rings so that both linear chains and rings may coexist and compete for the monomers. In Fig.6 we present the MWD of rings  $c_0(N)$  and of linear chains  $c_1(N)$  at density  $\phi = 1.5$  and  $E = 7$ . The linear chains appear to be unaffected by the presence of rings and scale, as before,  $c_1(N) \propto \exp(-\mu N)$  where the slope  $\mu$  is given by the inverse of the mean mass of the *linear* chains  $N_1$ . This can be easily understood by generalizing the

Flory-Huggins expression eq.(5) as a sum over the two different species  $s = 0, 1$ . The two different MWD decouple and the functional derivation with respect to both yields simply  $c_s(N) = \exp(-f_{chain}^s(N, \phi, E) - N\mu)$  for both species in analogy with eq.(6). The free energy of the linear chain is  $f_{chain}^1 = E + 1 + f_{end}$  as before. In the strong overlap regime  $f_{end}$  becomes again independent of mass  $N$  ( hence, the pure exponential seen for  $c_1(N)$ ) and, as a matter of fact, equals the density dependent value  $f_1(\phi)$  obtained for the purely linear systems which is tabulated in Tab.II. Therefore the mean mass of linear chains determines once again the chemical potential  $\mu$ .

However, our systems of *flexible* rings appear to be ring dominated, i.e. much more monomers are contained in closed loops than in linear chains, as expected. In contrast in systems of semi-flexible polymer chains the formation of rings is going to be strongly suppressed [12]. The MWD of rings is not exponential, but rather shows a clearly pronounced power law behavior  $c_0(N) \propto N^{-\tau}$  where  $\tau = 2.5$ . (This does not exclude, however, a final exponential cut-off, which can hardly be detected because of the dominating power law.) The exponent  $\tau$  can be obtained by a simple argument due to Porte [11]. The ratio of both MWD gives the ratio of the two partition functions  $Z_s$

$$\frac{c_0(N)}{c_1(N)} = \frac{Z_0(N)}{Z_1(N)} = \exp(f_{chain}^1 - f_{chain}^0). \quad (9)$$

The ratio  $Z_1/Z_0$  is equal to the probability of opening a loop, which must be proportional to: (i) the Boltzmann weight,  $\exp(-E)$ , due to the constant scission energy, (ii) the number of places where the ring can break,  $N$ , and (iii) the volume  $R^D \propto N^{D\nu}$  that two neighboring segments can explore after being disconnected ( $D$  denotes the dimension and  $\nu$  the relevant Flory exponent at density  $\phi$ ). Hence,  $c_0 \propto N^{-\tau} \exp(-N/N_1)$  with  $\tau = D\nu + 1 = 5/2$  at strong chain overlap in  $D = 3$ , and  $\tau = 2$  in  $D = 2$  where  $\nu = 1/2$ . Both exponents are well born out by the measured  $c_0$ -slopes depicted in the inset of Fig. 6. We compare here data we obtained with three different algorithms: OLMC, BFM and Grand Canonical Potts model (in 2D and 3D). The exponents in both dimensions are fully consistent with the predicted ones.

We return now again to systems containing linear chains only.

## V. THE SCALING OF THE AVERAGE CHAIN MASS

So far we have reported on the general form and scaling of the MWD. Now we want to go further and to investigate the scaling of the average chain mass and the second moment, i.e. the polydispersity index  $I = \langle N^2 \rangle / \langle N \rangle^2$ , with regard to density  $\phi$  and scission energy  $E$  (see Tab.I).

In the high density limit, i.e. within the validity of eq.(7), the inverse Lagrange multiplier equals the mean-chain length as mentioned above and the polydispersity  $I = 2$ . From the normalization constraint  $\phi = \sum_N N c(N)$  one infers that the mean mass is generally given by

$$\langle N \rangle = \mu^{-1} = \sqrt{\phi \exp(E + f_{end}(\phi))}. \quad (10)$$

For semi-dilute polymer chains one obtains from eq.(10) and eq.(8)  $\langle N \rangle \propto \sqrt{\phi^{1+(\gamma-1)/(3\nu_I-1)} \exp(E)}$  in agreement with the exponents  $\alpha_{II} \approx 0.6$  and  $\delta_{II} = 1/2$  quoted in the Introduction. Similarly, one finds in the dilute limit  $\alpha_I = \delta_I = 1/(1 + \gamma) \approx 0.46$  [1].

In Fig.7 we have plotted  $\langle N \rangle$  versus  $E$  to check for the expected  $\exp(\delta E)$  behavior. Despite the small difference in both values one distinguishes for dilute systems a slope with  $\delta_I = 0.46$  and for the dense system ( $\phi = 1$ )  $\delta_{II} = 0.5$ . One can verify on Fig.7 that at concentration  $\phi = 0.125$  a crossover into the semi-dilute regime for  $E \approx 9$  occurs whereby the slope of the exponential function changes from  $\delta_I \approx 0.46$  to  $\delta_{II} = 1/2$ , i.e. the isolated polymer coils get large enough so they start touching each other. At  $\phi = 0.25$  the concentration is already sufficiently high so this happens at comparatively lower energies  $E > 5$ . The  $\delta_{II} = 1/2$ -slopes confirm that at high densities  $f_{end}$  becomes chain length-independent and that eq.(10) holds. This scaling prediction is verified explicitly in Fig.8 where we have plotted  $\langle N \rangle$  versus the scaling variable indicated by eq.(10). Here we have used the values  $f_1(\phi, E)$  determined directly from the MWD. A plot using the prediction for

semi-dilute polymers eq.(8) is, however, *not* successful for  $\phi > 0.5$ . Hence, the measured  $f_1$  encapsulates physics other than the one expected in the limit of large blobs. To corroborate this further we plot in Fig.9  $u = \langle N \rangle^2 / (\phi \exp(E))$  versus  $\phi$ . From eq.(10) we know that  $u = \exp(f_{end})$  for strong overlap. Not surprisingly the data collapse in that limit, but not the dilute systems. (This will be improved in Fig.10, see below.) Also indicated are the  $f_1$  (stars) directly estimated from the MWD in the strong chain overlap limit. Notably, for  $\phi \geq 0.5$  the mean mass appears to increase much faster than the growth exponent  $\alpha_{II} = 0.6$ . This breakdown of eq.(8) — but not of eq.(10) — is not unexpected if one bears in mind that the scaling arguments can only be valid in the limit [4] of  $\phi \rightarrow 0$  and  $g \rightarrow \infty$ , i.e. when the blob is larger enough. This result suggests to rewrite eq.(8) as a systematic series expansion

$$f_{end}(\phi) = B_{-1} \log(\phi/\phi_0) + B_1 \phi + \dots \quad (11)$$

where in order to match semi-dilute and melt regime we choose  $B_{-1} = (\gamma - 1)/(3\nu_I - 1) \approx 2.1$  and  $\phi_0 \approx 0.018$ . The fit using eq.(11) with  $B_1 \approx 0.8$ , depicted in Fig.9, is only qualitatively satisfactory and further study is warranted. The above expansion is motivated by a recent second virial theory on wormlike micelles and rigid rods interacting via hard-core excluded volume [8]. The applicability of this theory to our systems of *flexible* EP with persistence length  $b$  of order of the sphere diameter (see Tab.II) appears to be unclear. Nevertheless, it is interesting to note that the second virial coefficient  $B_1 = 8/3 v \approx 0.6$  predicted in [8] is relatively close to the constant measured. Alternatively, the dependence of  $\langle N \rangle$  on  $\phi$  might be represented by an effective growth exponent  $\alpha_{eff} \approx 1$  (dotted line). These values agree also favorably with an earlier lattice simulation [2] although this is presumably accidental due to the different microscopic physics which must intervene.

A proper crossover scaling between dilute and semi-dilute regimes (but not with regard to the molten regime) is achieved by plotting  $\langle N \rangle / N^*$  versus  $\phi / \phi^*$  in Fig.10. The crossover length  $N^* \propto \exp(-\varphi E)$  with  $\varphi = (1/2 - \alpha_I)/(\alpha_{II} - \alpha_I) \approx 0.26$  and the crossover density  $\phi^* \propto \exp(\kappa E)$  with  $\kappa = \alpha_I(1 - \varphi) \approx 0.34$  are readily found by matching the asymptotic

behaviors of the dilute and semi-dilute regime. We have included data from both OLMC and the BFM. For clarity, the BFM data have been shifted downwards by a factor 10. As one anticipates from Fig.9, only OLMC data for  $\phi \leq 0.5$ , i.e. volume fractions smaller 0.1 collapse properly on the predicted asymptotes — confirming hence the polymer physics expressed in eq.(8) — while at higher densities simple liquids physics becomes relevant.

## VI. SUMMARY

We have proposed here a new off-lattice Monte Carlo algorithm (OLMC) for systems of equilibrium polymers (EP). It is shown that this model faithfully reproduces the results of ref. [1]: the MWD of linear EP is essentially exponential even in the limit of very high density in contrast to recent claim [2]. Note that our findings do not support recent claims of Levy-flight dynamic behavior in EP and GM which would require a singularity in the MWD of linear chains [7].

If ring formation is allowed, however, the MWD for rings alone is strongly singular,  $c_0(N) \propto N^{-\tau}$  with  $\tau = D\nu + 1$ . This result has been confirmed both in two- and in three dimensions for different lattice and off-lattice models. We have also shown that the MWD of linear chains is not affected by the presence of rings in the system which demonstrates that the general Flory-Huggins approach is very accurate even in this case.

The mean chain length of linear EP is found to vary with density  $\phi$  and scission energy  $E$  like  $\langle N \rangle \propto \phi^\alpha \exp(\delta E)$  as observed in our earlier Bond Fluctuation Model investigation [1] with exponents  $\alpha_I = \delta_I \approx 0.46$  in the dilute regime and  $\alpha_{II} = 0.6, \delta_{II} = 0.5$  in the semi-dilute regime. This holds only for volume fractions smaller 0.1.

At higher densities when the blobs become too small the scaling approach breaks down. Conformational properties are then largely determined by packing effects as in simple liquids. The mean chain length then grows much faster with  $\phi$ , qualitatively following a nonalgebraic dependence similar to a recent description put forward for rod-like and semi-flexible micelles [8]. Our result is also compatible to an effective growth exponent  $\alpha_{eff} \approx 1$ , in agreement

with recent simulations [2] and even with experimental observations [19] although in the latter case this agreement might be accidental in view of the rather low volume fraction probed experimentally.

As a further development the OLMC algorithm the model will be used for studies of the dynamic behavior of linear and ring EP for which investigations are currently underway.

### **ACKNOWLEDGMENTS**

This research has been supported by the National Science Foundation, Grant No. INT-9304562 and No. DMR-940518, and by the Bulgarian National Foundation for Science and Research under Grant No. X-644/1996. JPW thanks J.L. Barrat, L. Bellier-Castella, M.E. Cates, Y. Rouault and P. van der Schoot for stimulating discussions.



# TABLES

$\phi$	$E$	$\langle N \rangle$	$I$	$R_e$	$R_g$	$\phi/\phi^*$
0.125	8	25	1.86	6.4	2.5	0.3
0.125	9	42	1.88	8.7	3.4	0.5
0.125	10	66	1.89	12.2	4.5	0.7
0.125	11	108	1.93	14.8	5.9	1.0
0.125	12	181	1.95	19.9	8.0	1.5
0.25	7	24	1.88	6.0	2.4	0.6
0.25	8	38	1.90	7.9	3.2	0.9
0.25	9	63	1.93	10.4	4.2	1.2
0.25	10	102	1.93	13.6	5.5	1.7
0.25	11	166	1.92	17.5	7.1	2.3
0.25	12	270	1.99	23.1	9.3	3.1
0.5	7	38.4	1.92	7.9	3.2	1.8
0.5	8	62	1.94	10.3	4.2	2.5
1	5	28	1.92	5.8	2.3	1.9
1	6	46	1.94	7.5	3.0	2.5
1	7	74	1.94	9.6	3.9	3.4
1	8	123	1.96	12.7	5.2	4.8
1.38	7	105	1.97	10.9	4.5	5.0
1.5	6	73	1.95	8.6	3.6	4.0
1.5	7	120	1.97	10.6	4.6	5.1

TABLE I. Summary of measured quantities for configurations with  $\langle N \rangle > 20$ . Quantities tabulated: the mean chain mass  $\langle N \rangle$ , the polydispersity index  $I = \langle N^2 \rangle / \langle N \rangle^2$ , the mean end-to-end distance  $R_e$  the mean gyration radius  $R_g$ , and the chain overlap  $\phi/\phi^*$ . Note that  $I$  increases systematically with chain overlap.

$\phi$	$l$	$b$	$\xi$	$f_1$
0.125	0.7574	1.41	4.7	0.4
0.25	0.7565	1.33	4.0	0.65
0.5	0.7530	1.2	3.8	0.9
1.0	0.7408	1.12	3.3	1.66
1.38	0.7234	1.05	2.8	1.97
1.5	0.7158	1.02	2.5	2.21

TABLE II. Density dependence of mean bond length  $l = \langle l^2 \rangle^{1/2}$ , the persistence length  $b$  for Gaussian chains of blobs, the blob size  $\xi$  estimated from the slopes in Fig.2, and the free energy factor  $f_1(\phi)$  obtained from the exponential tail of the MWD as explained in Sec.IV.

## REFERENCES

- [1] J. P. Wittmer, A. Milchev, and M. E. Cates, J.Chem. Phys., **109**, 834 (1998).
- [2] Y. Rouault, Phys. Rev. E, **58**, 6155 (1998).
- [3] The physical properties of EP and specifically GM have been reviewed briefly in [1] and more extensively in M. E. Cates and S. J. Candau, J. Phys. Cond. Matt. **2**, 6869 (1990). In ref. [1] we also review and analyze some of the older computational work on EP.
- [4] P.G. de Gennes, *Scaling Concepts in Polymer Physics*, Cornell Univ. Press, Ithaca (1979); J. des Cloizeaux and G. Jannink, *Polymers in Solution*, Clarendon Oxford (1990).
- [5] I. Carmesin and K. Kremer, Macromolecules, **21**, 2819 (1988).
- [6] S. Caracciolo, M.S. Causo, A. Pelissetto, Phys. Rev. E, **57**, R1215 (1998).
- [7] A. Ott, J. P. Bouchaud, D. Langevin and W. Urbach, Phys. Rev. Lett. **65**, 2201(1990).
- [8] P. van der Schoot and M. E. Cates, Langmuir **10**, 670(1994).
- [9] A. Milchev, J.P. Wittmer, and D.P. Landau Europ. Phys. J. B, in print; cond-mat/9905336.
- [10] A. Milchev, J.P. Wittmer, and D.P. Landau, J.Chem.Phys., submitted for publication, 1999.
- [11] Porte G., in *Micelles, Membranes, Microemulsions, and Monolayers*, edited by W.M. Gelbart, A. Ben-Shaul and D.Roux (Springer-Verlag, New York) 1994.
- [12] P. van der Schoot, J.P. Wittmer, Makromolekulare Chemie – Theory and Simulations, accepted May 1999; cond-mat/9808175.
- [13] This problem does not arise for an algorithm with artificial dynamics like the Potts mapping of EP problem proposed earlier (A. Milchev and D. P. Landau, Phys. Rev. E

- 52**, 6431 (1995)) where the EP chains are mapped on spin states on a lattice and the chain connectivity is fictitious.
- [14] I. Gerroff, A. Milchev, W. Paul, and K. Binder, J. Phys. Chem. **98**, 6526 (1993);  
A. Milchev, W. Paul, and K. Binder, J. Phys. Chem. **99**, 4786 (1993).
  - [15] A. Milchev and K. Binder, Macromolecules, **29**, 343 (1996).
  - [16] P.N. Pusey, in *Liquids, Freezing and Glass Transition*, Les Houches 1989, J.P. Hansen, D. Levesque and J. Zinn-Justin, eds., North-Holland (1991).
  - [17] More generally,  $f_{chain}$  might even depend explicitly on  $c(N)$ . This is of relevance in situations such as LP brushes where the MWD is conjugated with the density profile of the layer [10].
  - [18] Minor corrections to Eq.(8) from the small fraction of chains that are too long for their excluded-volume interactions to be screened by the surrounding chains (under melt conditions this applies [4] to those chains whose length exceeds  $\langle N \rangle^2$ ). However, this contribution is exponentially small and can be neglected.
  - [19] P.Schurtenberger, C.Cavaco, F.Tilberg, and O.Regev, Langmuir, **12**, 2894 (1996).

# FIGURES

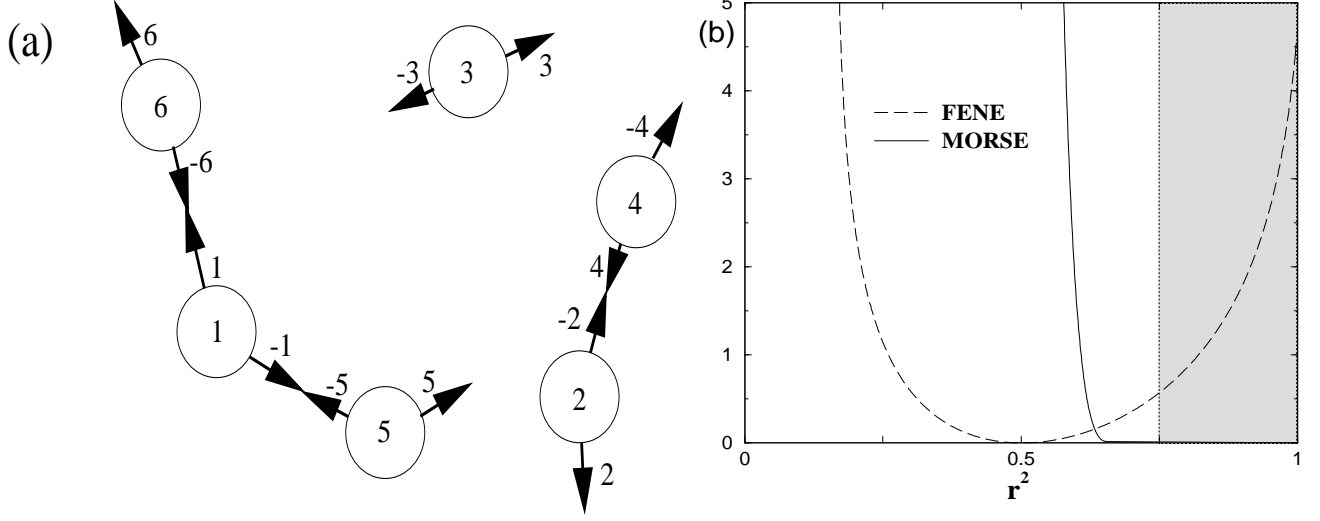


FIG. 1. Sketch of algorithm: (a) Bonds between spherical beads break and recombine constantly with rates depending on the scission energy  $E$  which is assumed independent of mass  $N$  and number density  $\phi$ . Each monomer has two (saturated or unsaturated) bonds. Chains consists of symmetrically connected lists of bonds. The data structure is based on the bonds rather than the polymer chains. (b) Plots of bonded (FENE) and non-bonded (Morse) interactions used in the present model. The shaded area denotes distances where scission - recombination events may take place.

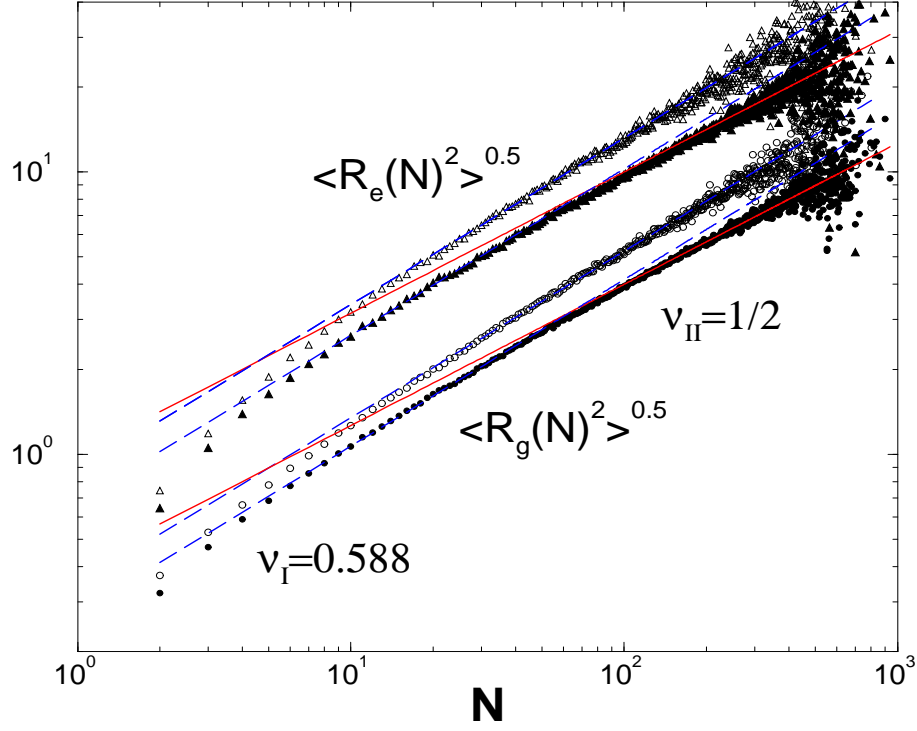


FIG. 2. Variation of the end-to-end distance  $R_e$  (triangles) and the radius of gyration  $R_g$  (squares) with chain mass  $N$  at  $E = 7$  for dilute (open symbols:  $E = 7, \phi = 0.125$ ) and concentrated (full symbols:  $E = 7, \phi = 1$ ) systems. The dashed lines denote the dilute exponent  $\nu_I = 0.588$  which is visible for the dilute systems over the full range of  $N$  and for the semi-dilute system for small  $N$ , i.e. within the blob. The slope  $\nu_{II} = 1/2$  indicates the Gaussian statistics for strongly overlapping long chains.

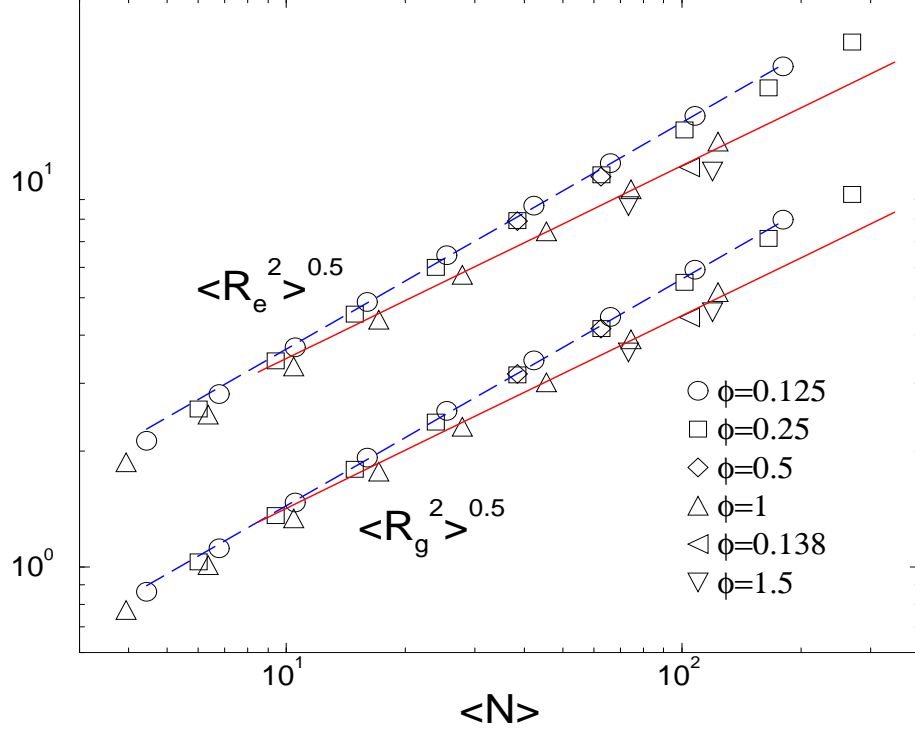


FIG. 3. End-to-end distance  $R_e$  and radius of gyration  $R_g$  vs. mean chain mass  $\langle N \rangle$ . At small density ( $\phi = 0.125, 0.25$ ) and, hence, weak chain overlap the chains are swollen (dashed line). At high density and mass we obtain Gaussian statistics (solid lines).

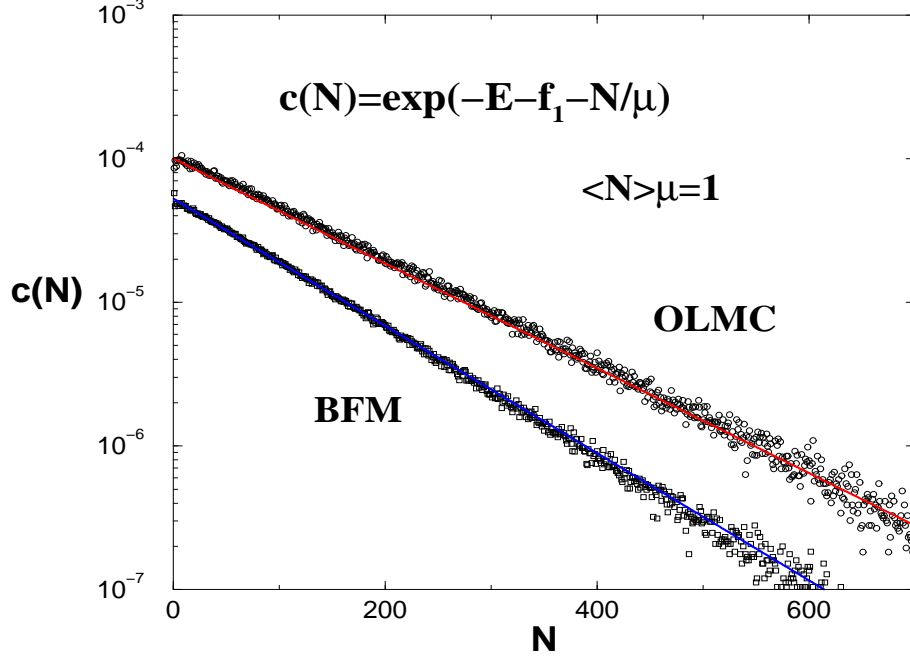


FIG. 4. MWD  $c(N)$  versus  $N$  at high density for OLMC (upper curve;  $E = 7, \phi = 1.5$ ) and BFM (lower curve;  $E = 7, 8\phi = 0.5$ ) systems. Note that the distribution is always a pure exponential and *no* sign of singularity was found for whatever density or energy. These curve are used to fit  $f_1$ . For OLMC we have  $\langle N \rangle \approx 119$ ,  $f_1 \approx 2.21$ , for BFM  $\langle N \rangle \approx 98$ ,  $f_1 \approx 2.85$ .



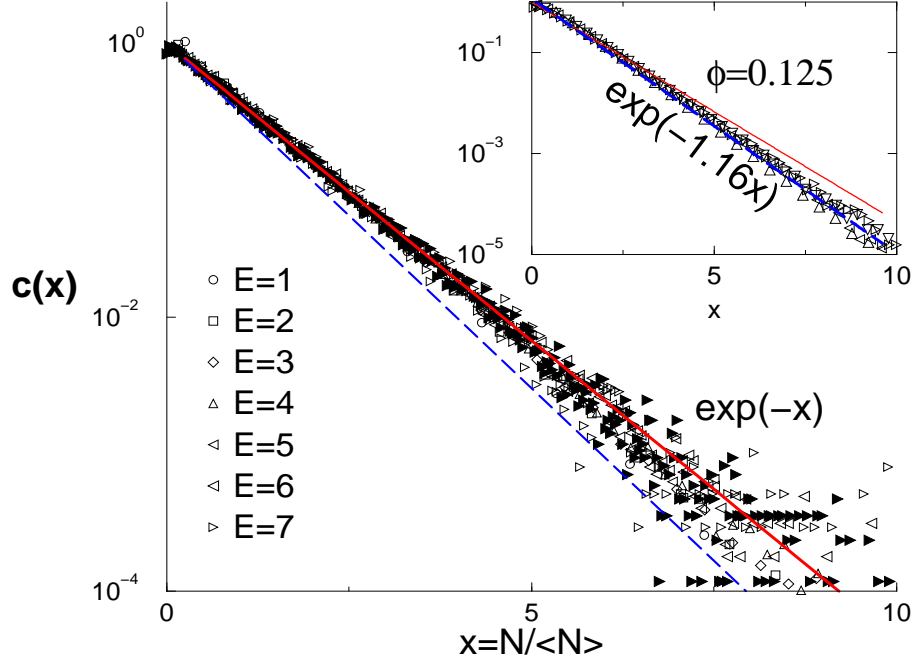


FIG. 5. Data collapse of (properly normalized) MWD  $c(x)$  versus  $x = N/\langle N \rangle$  for OLMC. In the main figure the high density scaling prediction  $c(x) = \exp(-x)$  is verified (full line). The open symbols denote density  $\phi = 1$  and the full symbols  $\phi = 1.5$ . Inset: The MWD in the dilute limit (OLMC at  $\phi = 0.125$ ) compares well with the prediction  $c(x) \propto \exp(-\gamma x)$  (dashed line). The same symbols are used as in the main figure.

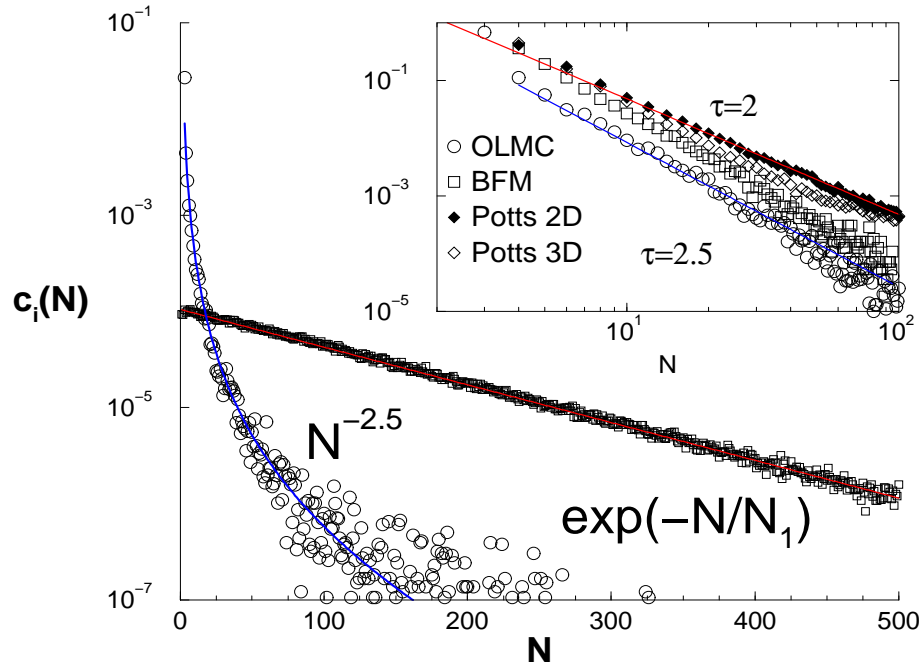


FIG. 6. MWD for mixed systems containing rings. Main figure:  $c_0$ -MWD of rings (spheres),  $c_1$ -MWD of linear chains (squares). Inset: Ring MWDs for different models and dimensions. The indicated slopes confirm  $\tau = 5/2$  in 3D and  $\tau = 2$  in 2D.

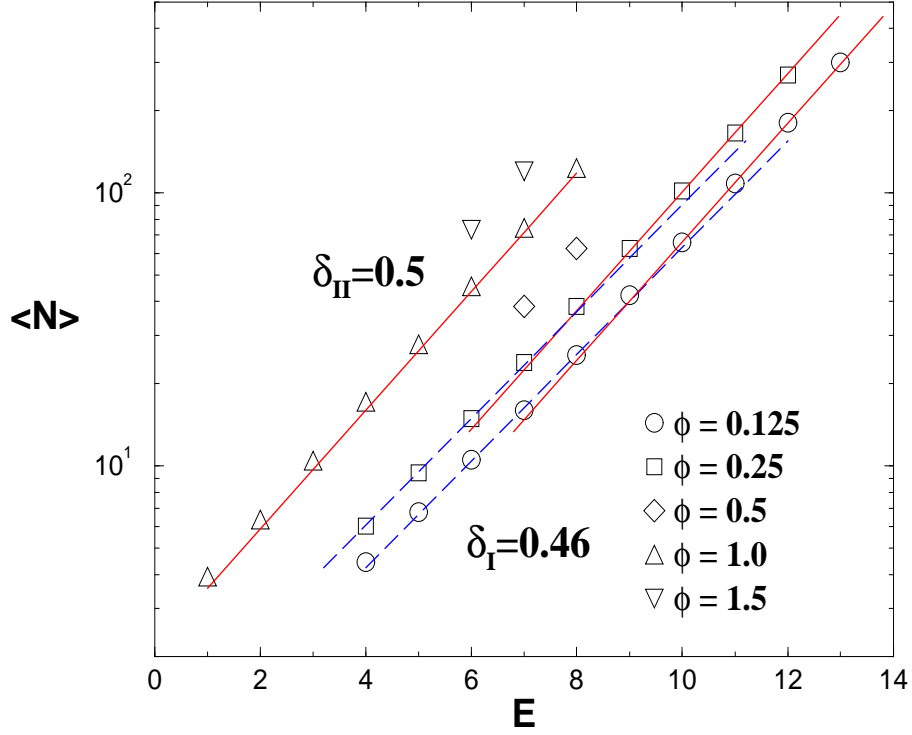


FIG. 7. Variation of mean chain mass  $\langle N \rangle$  with dimensionless bond energy  $E$  for various number densities  $\phi$  as indicated in the figure. At low chain overlap the data are consistent with the exponent  $\delta_I = 0.46$  (dashed lines), at high density with the mean field exponent  $\delta_{II} = 0.5$  (full lines).

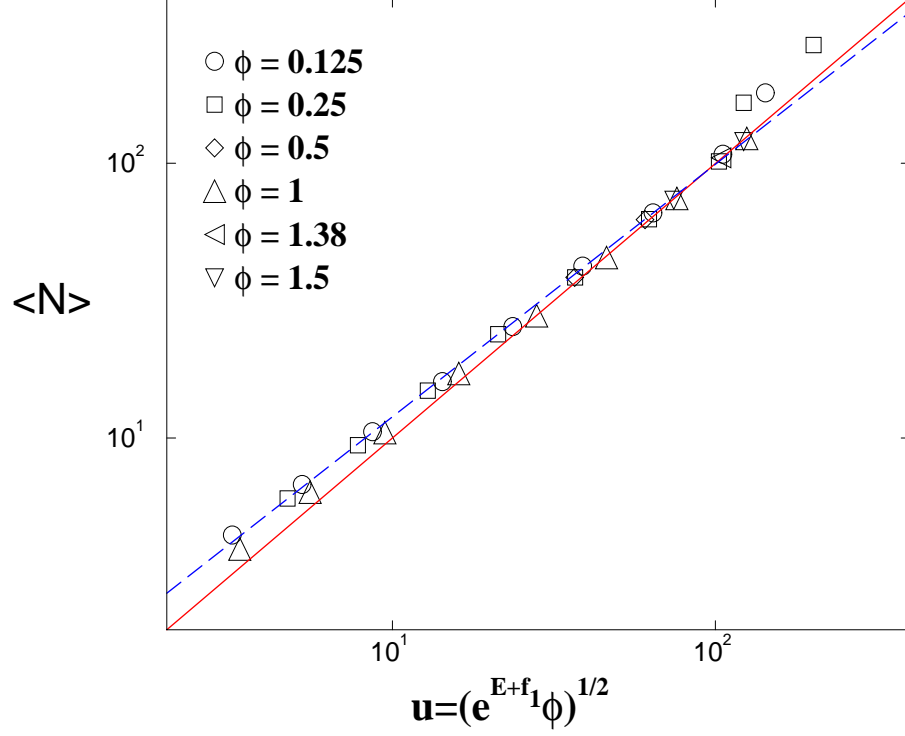


FIG. 8. Scaling attempt in the high density limit for  $\langle N \rangle$ . The collapse confirms the scaling with respect to  $u$  in the high chain overlap limit and the  $f_1$  obtained independently from the MWD  $c(N)$ . Note that the remarkable good scaling works even in the dilute limit. The dashed line marks for comparison the dilute exponent  $\alpha_I$ .

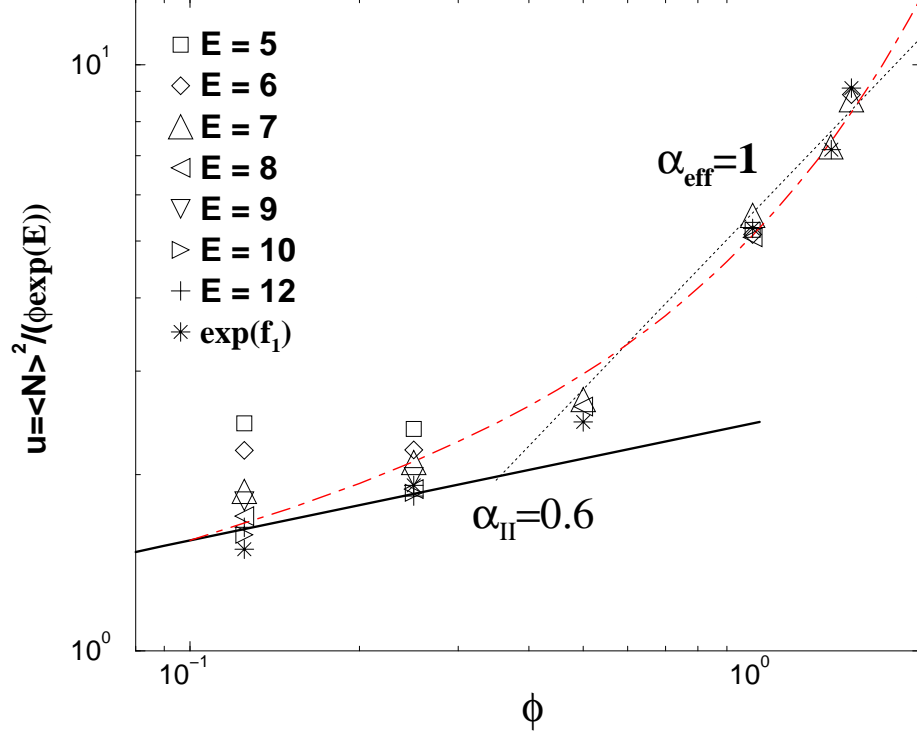


FIG. 9. A crude rescaling attempt of mean chain mass  $u = \langle N \rangle^2 / (\phi \exp(E))$  versus  $\phi$ . Also indicated are the  $\exp(f_1)$  estimated from the MWD (stars). The mean chain mass rises faster for large densities  $\phi \geq 0.5$ . This regime is compared with an effective exponent  $\alpha_{eff} \approx 1$  (dotted line) and the nonalgebraic density dependence eq.(11) with  $B_{-1} = 0.21$  and  $B_1 \approx 0.8$  (dashed-dotted line).

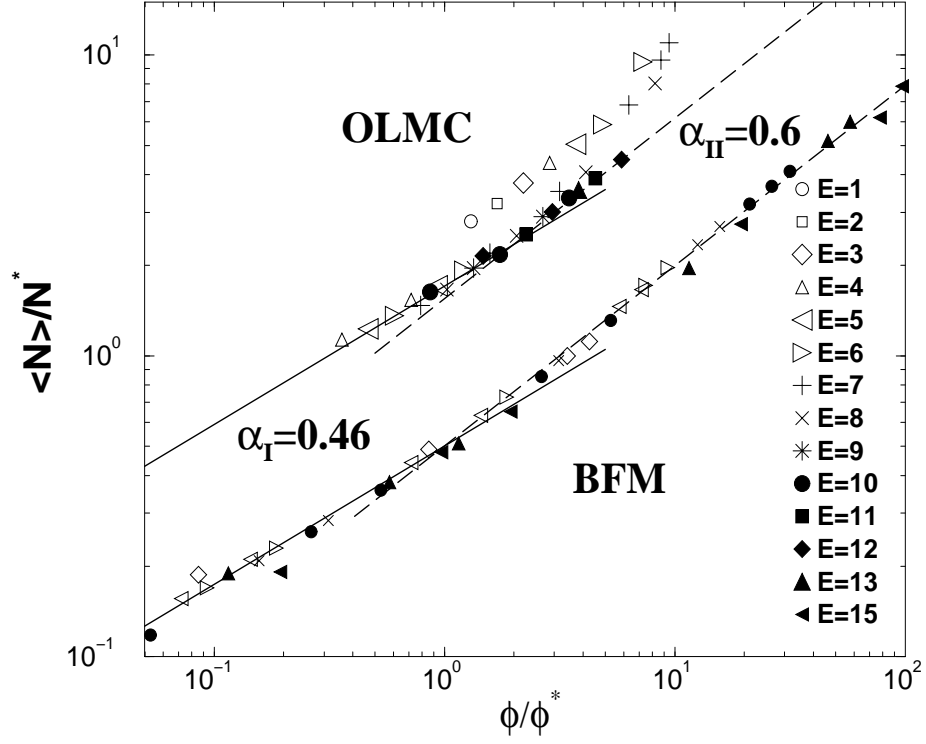


FIG. 10. Dilute-Semidilute crossover scaling  $\langle N \rangle / N^*$  vs.  $\phi / \phi^*$  for OLMC and BFM (shifted downwards for clarity). For densities  $\phi \geq 0.5$  the OLMC data do not scale and are systematically above the semi-dilute asymptote. This is due to additional entropic interactions between the dense beads which increases the mean chain mass.